

Supplementary Information

Linker scissoring strategy enables precise shaping of Fe/Mn-MOF to construct S-scheme heterojunction with Bi₂S₃ for enhanced photoexcitation under peroxymonosulfate activation

Ronghua Zhang,^{ab} Zaikun Xue,^b Jiaxin Shao,^c Zhaolong Li,^b Hao Liang,^a Qingshan Li^a and Ning Yuan^{*a}

^a School of Chemical and Environmental Engineering, China University of Mining and Technology, Beijing 100083, China

^b Beijing Graphene Institute, Beijing 100095, China

^c School of Materials Science and Engineering, Peking University, Beijing 100871, China

* Corresponding author: Ning Yuan, E-mail: ning.yuan@cumtb.edu.cn

Text S1 Experimental section

S1.1. Chemicals

All reagents and solvents were used commercially without further purification. The following reagents, including thioacetamide (TAA, C₂H₅NS), bismuth nitrate pentahydrate (Bi(NO₃)₃·5H₂O), iron chloride hexahydrate (FeCl₃·6H₂O, 99%), 2-amino terephthalic acid (NH₂-H₂BDC), tetracycline hydrochloride (TC), *tert*-butyl alcohol (TBA, 99%), 2,2,6,6-tetramethylpiperidine-1 oxy radical (TEMPO, 98%), potassium iodide (KI), *p*-benzoquinone (*p*-BQ), dibasic sodium phosphate (Na₂HPO₄), sodium bicarbonate (NaHCO₃), sodium sulfate (Na₂SO₄), sodium chloride (NaCl), sodium nitrate (NaNO₃), *N,N*-dimethylformamide (DMF, 99.5%) and peroxymonosulfate (2KHSO₅·KHSO₄·K₂SO₄, PMS) were supplied by Macklin Chemical Reagent Co., Ltd (Shanghai, China). Manganese acetate tetrahydrate (Mn(CH₃COO)₂·4H₂O) was acquired from Tianjin Damao Chemical Reagent Factory. Sodium hydroxide (NaOH), hydrochloric acid (HCl, 36–38%), sodium sulfate (Na₂SO₄) and anhydrous ethanol (CH₃CH₂OH, AR) were purchased from the Sinopharm Chemical Reagent Co., Ltd. Nafion was obtained from Shanghai Chemical Technology Co. Methanol (MeOH) was offered by Beijing InnoChem Science & Technology Co., Ltd. ITO glass substrates were obtained by OPV TECH Co., Ltd.

S1.2. Characterization

The crystal structure and crystallinity were analyzed by powder X-ray diffraction (XRD) measurements on Bruker D8 advance X-ray diffractometer (Germany) with monochromatized Cu K α radiation ($\lambda = 0.15406$ nm) at 40 kV and 40 mA and the data was collected in a range of 5 to 90° with scanning speed of 4°/min and step size of 0.02°. The chemical functional groups were examined on a Fourier transform infrared spectrometer (FT-IR, Shimadzu IRTracer-100, Japan) over a range of scanning 400–4000 cm⁻¹ with 32 sweeps at 4 cm⁻¹ intervals. Field emission scanning electron microscope (SEM, FEI Quattro S, USA) collocation with an energy-dispersive X-ray detector (EDS, AMETEK Digiview 5, USA) was employed to investigate the

morphologies and elemental composition at 10 kV and 46 pA. The microstructure was recorded by a high-resolution dark-field scanning transmission electron microscope (TEM, FEI Tecnai G2 F20, USA) instrument operating at 200 kV. The surface elemental analysis and chemical states were tested by X-ray photoelectron spectroscopy (XPS, FEI ESCALAB 250Xi, USA) with a monochromatic Al K α X-ray source with C1 s at 284.6 eV. The pore diameter distribution and specific surface area were performed on N₂ adsorption-desorption isotherms (BELSORP-max, Japan) at 77 K. Before testing, the samples were vacuum heat treated at 120 °C for 10 h to remove any adsorbed impurities or moisture. The UV-Vis diffuse reflectance spectra (UV-Vis DRS, Perkin Elmer Lambda 950, USA) were measured with BaSO₄ as a reference in the range of 200–800 nm at a scan speed of 266.75 nm/min with 2 nm intervals. The fluorescent signal intensity was collected via photoluminescence emission spectroscopy (PL, F-2700, Japan) with a 150 W Xe lamp at 327 nm as the excitation wavelength. Three-dimensional excitation-emission matrix fluorescence spectra (3D EEMs) were measured by an F-2700 spectrofluorometer, describing the scanning parameters of the excitation wavelengths (λ_{ex}) of 250–350 nm and the emission wavelengths (λ_{em}) of 360–500 nm with a scan speed of 1500 nm/min on the fluorescence intensity, respectively.

S1.3. Photoreaction procedures

An experimental solution with 5 mg catalysts and 20 mg L⁻¹ tetracycline was generated in a 50 mL quartz tube and ultrasonically dispersed for 1 h dark adsorption to ensure that the synthesized catalysts and tetracycline contaminant achieved adsorption equilibrium. The temperature was maintained at room temperature and a magnetic stirrer (600 rpm) was applied to attain well-mixed conditions. Photocatalysis experiments were performed under simulated sunlight using a 300 W Xe lamp regulated with a cut-off filter ($\lambda > 420$ nm). Followingly, 3 mL of suspension was extracted in 5 min intervals while being exposed to light, and then the mixture was centrifuged for 5 min at 10000 rpm. To obtain the residual mixture concentration in the filtered supernatant, the UV-Vis spectrophotometer (UV-N500, Yoke, China) was operated at a wavelength of 359 nm. The diluted NaOH and HCl

(0.1 mol L⁻¹) solvents were added to the mixture to regulate the target acid and alkaline conditions when performing a series of pH influence experiments.

The photocatalytic degradation efficiency was calculated using equation (1):

$$\eta = \frac{C_0 - C_t}{C_0} \times 100\% \quad (1)$$

where η is the degradation efficiency, C_0 is the initial TC concentration and C_t is the equilibrium concentration at t min degradation.

The pseudo-first-order reaction kinetic curves were used to acquire the reaction rate for different catalyst concentrations in photodegradation experiments. The kinetic equation (2) is calculated as:

$$-\ln(C_t / C_0) = kt \quad (2)$$

where k is the apparent rate constant.

After the photodegradation reaction, the ethanol and deionized water were used to clean the recycled catalysts several times for stability and repeatability tests and dried overnight at 60 °C for the next cycle.

S1.4. Electrochemical analysis

The photoelectrochemical property was determined by electrochemical impedance spectroscopy (EIS), linear sweep voltammetry (LSV), mott-Schottky plots (MS), and photocurrent response curve via an electrochemical apparatus (CHI 760E, Shanghai, China). The photoelectrochemical analysis was carried out in 0.5 M Na₂SO₄ electrolyte solution with a three-electrode system, including a saturated calomel electrode (SCE) as citation electrode, a Pt as counter electrode and a working electrode. The working electrode was prepared by 5mg catalyst, 50 μ L 1% Nafion diluent and 500 μ L ethanol were evenly mixed and sonicated for 10 min. Subsequently, 40 μ L dispersion was extracted in a 1 cm \times 2 cm indium-tin-oxide (ITO) glass, dried naturally overnight then placed in an oven at 70 °C for 2 h. During the assessment, photocurrent responses were tested on a 500 W Xe arc lamp (PLX300D, Beijing) with 40 s several light/dark irradiation cycles. EIS was collected in an alternating voltage of 5 mV. MS were based on frequencies of 800, 1000 and 1200

Hz in open-circuit voltage. LSV tests were selected with bias voltages from -1 to 1 V at the rate of 0.05 v s⁻¹.

S1.5. Response surface methodology

To evaluate the effect of four anions Cl⁻, SO₄²⁻, NO₃⁻ and HCO₃⁻ (labeled as A, B, C and D) on the photocatalytic degradation of TC, response surface methodology (RSM) was employed. A total of 29 groups experimental groups were simulated based on the Box-Behnken orthogonal design, using single-factor variables divided into three levels (-1, 0, +1). The detailed data are presented in Table S1. The four ion concentration values were referred to in the report literature.²⁵ The secondary function as well as the analysis of variance (ANOVA) was chosen to assess the response surface models through a Design-Expert® software (Minneapolis, USA). A polynomial regression modeling evaluated the response variable about degradation efficiency (%) and anionic types. The fitted second-order polynomial was calculated using Eq. 3:

$$Y = \beta_0 + \beta_1A + \beta_2B + \beta_3C + \beta_4D + \beta_{12}AB + \beta_{13}AC + \beta_{14}AD + \beta_{23}BC + \beta_{24}BD + \beta_{34}CD + \beta_{11}A^2 + \beta_{22}B^2 + \beta_{33}C^2 + \beta_{44}D^2 \quad (3)$$

where Y relates to the optimal degradation efficiency (%) (response), β_0 is the intercept coefficient, $\beta_1, \beta_2, \beta_3$ and β_4 relates to independent variable coefficients, $\beta_{11}, \beta_{22}, \beta_{33}$ and β_{44} represent quadratic terms, $\beta_{12}, \beta_{13}, \beta_{14}, \beta_{23}, \beta_{24}$ and β_{34} as interaction coefficients.

S1.6. Density function theory

The density functional theory (DFT) demonstrated the changes in the electronic structure of TC as a result of the attack of the catalytically active site by the reactive species via Gauss view (ver. 6.0). The Gaussian 09 with B3LYP/6-31 G* procedures optimized the geometrical structure to certify the frequency of occurrence of target pollutants. The Fukui index was calculated by Multiwfn 3.8 as the formula (Eq. 4-7):²⁶

$$f(r) = \left[\frac{\partial p(r)}{\partial N} \right]_{v(r)} \quad (4)$$

$$f^0(r) = \frac{f^+(r) + f^-(r)}{2} = \frac{q_{N+1}(r) - q_{N-1}(r)}{2} \quad (5)$$

$$f^-(r) = q_N(r) - q_{N-1}(r) \quad (6)$$

$$f^+(r) = q_{N+1}(r) - q_N(r) \quad (7)$$

where f^0, f^-, f^+ relate the radicals attack, electrophilic attack and nucleophilic attack in Fukui index. $q(r)$ represents the electron density at a point r and v denotes the external potential constant, N is the total number of electrons.

The atomic reactivity in TC molecules was conducted by condensed dual descriptor (CDD) as Eq. 8:²⁷

$$f^2 = f^+(r) - f^-(r) = 2q_N(r) - q_{N+1}(r) - q_{N-1}(r) \quad (8)$$

S1.7. Analytical methodology

Reactive oxygen species were examined by electron spin resonance (ESR) spectroscopy (A300-10/12, Bruker; Germany). The contribution of active species was assessed through trapping experiments using the quenching agents. The 5,5-dimethyl-pyrine-N-oxide (DMPO), DMPO-CH₃OH, and 2,2,6,6-tetramethylpiperidine (TEMP) quenching agents served as the spin-trapping solvents of •OH/•SO₄⁻, •O₂⁻ and ¹O₂, respectively. To investigate the primary active species in the degradation process, the MeOH for 1 mmol L⁻¹, TBA for 50 mmol L⁻¹, p-BQ for 1 mmol L⁻¹ and TEMPO for 1 mmol L⁻¹ as sacrificial agents were added to a mixture solvent and used to capture the target species for •SO₄⁻, •OH, •O₂⁻ and ¹O₂.

The photocatalytic degradation intermediates of tetracycline were estimated by a liquid chromatograph mass spectrometer (LC-MS/MS, LCMS-8040, Shimadzu, Japan). The 0.1% (v/v) formic dispersed in ultrapure water and acetonitrile were used as mobile phases A and B. The flow rate was 0.5 mL min⁻¹. The column temperature was 303 K. The 5 μL photodegradation solution was injected for the detection of intermediates to obtain m/z values. The relative results are detailed in Fig. S4.

Text S2 The analysis of SEM, XRD and LG-MS spectra

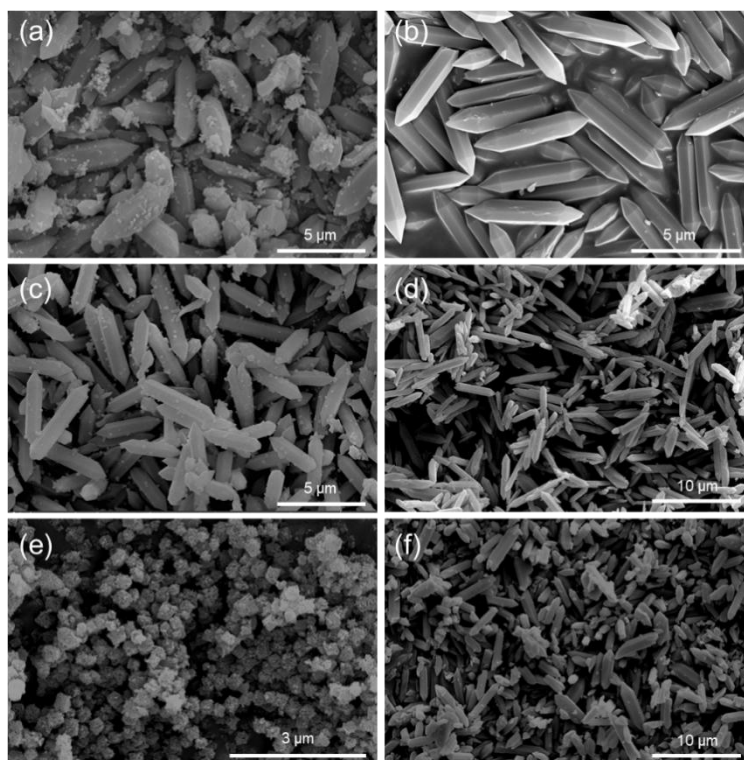


Fig. S1. The SEM images of (a) NF₄M₀, (b) NF₃M₁, (c) NF₁M₁, (d) NF₁M₃, (e) 2 mL of acetic acid-modulated NF₃Mc and (f) 5 mL of acetic acid-modulated NF₃Mc.

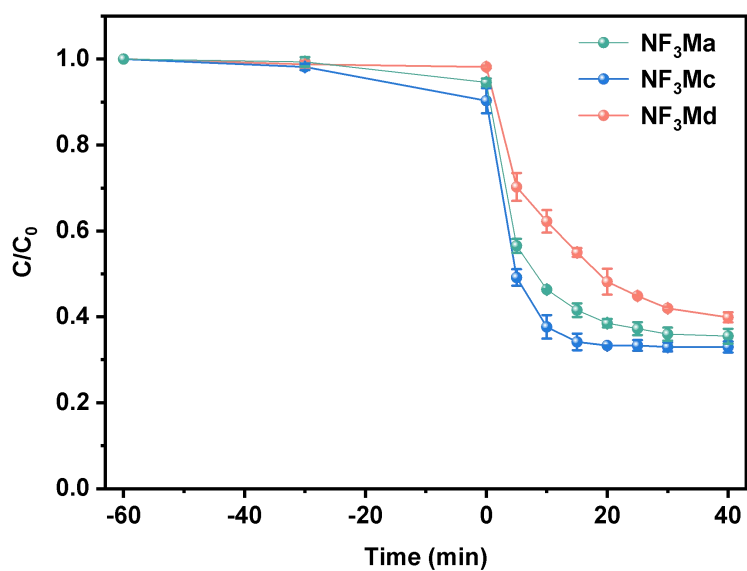


Fig. S2. The degradation efficiency of NF₃Ma (HPBC), NF₃Mc (QBC) and NF₃Md (HPC) for TC.

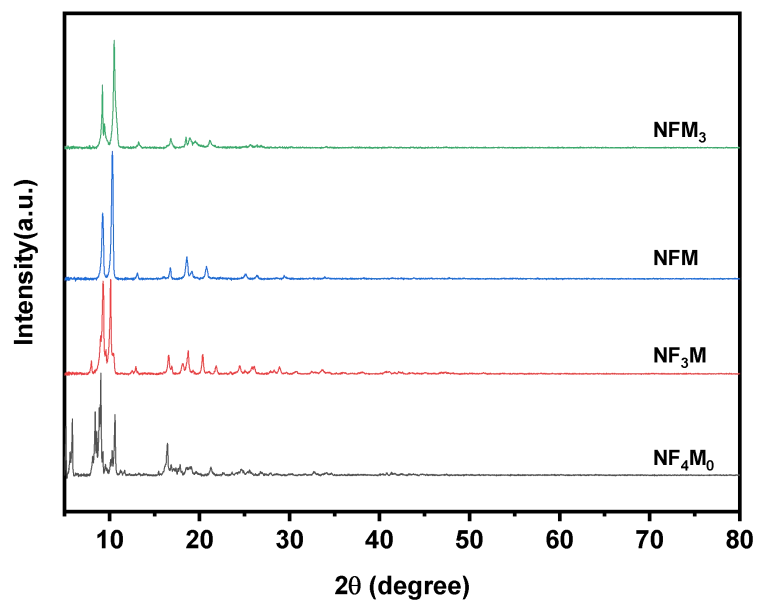


Fig. S3. The XRD patterns of NF_4M_0 , NF_3M , NFM and NFM_3 .

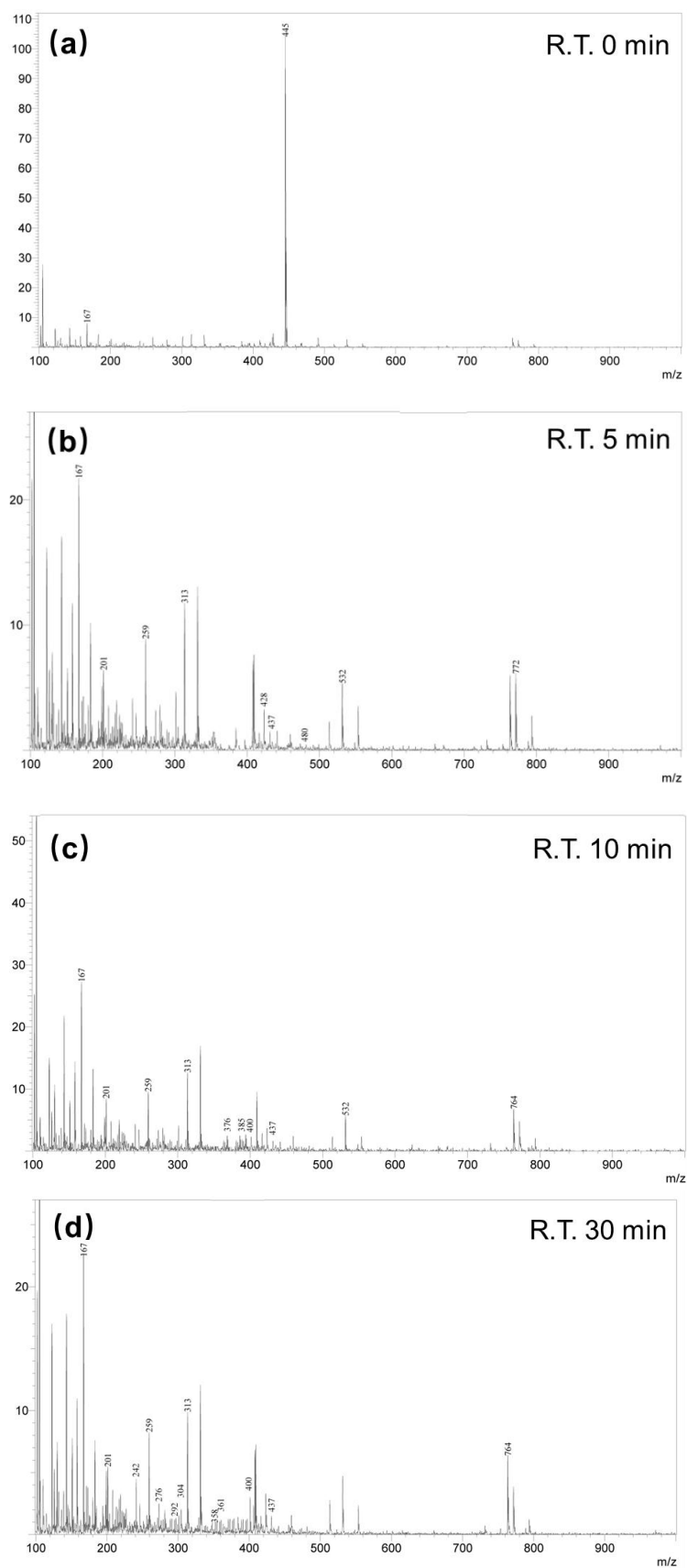


Fig. S4. The LG-MS spectra of TC intermediates at different degradation times (R. T. = reaction time).

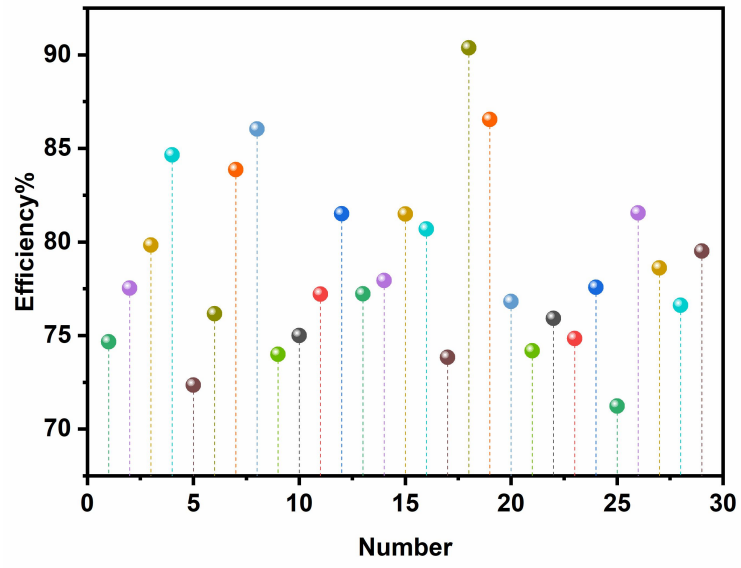


Fig. S5. The TC removal efficiencies of 29 experiments.

Text S3 Supplementary Tables

Table S1. The methodology data of response surface methodology.

Run	A	B	C	D	Efficiency
	(Cl ⁻ , mg L ⁻¹)	(SO ₄ ²⁻ , mg L ⁻¹)	(NO ₃ ⁻ , mg L ⁻¹)	(HCO ₃ ⁻ , mg L ⁻¹)	%
1	2800	80	0	11	74.67
2	1400	80	3.55	11	77.53
3	2800	80	3.55	0	79.84
4	1400	80	0	0	84.66
5	1400	80	0	22	72.35
6	1400	160	0	11	76.16
7	1400	80	7.1	0	83.86
8	0	0	3.55	11	86.03
9	2800	80	7.1	11	74
10	0	80	3.55	22	75
11	1400	80	3.55	11	77.21
12	1400	0	0	11	81.51
13	1400	80	3.55	11	77.23
14	1400	80	3.55	11	77.94
15	0	80	7.1	11	81.49
16	1400	160	3.55	0	80.69
17	2800	160	3.55	11	73.84
18	0	80	3.55	0	90.37
19	1400	0	3.55	0	86.55
20	2800	80	3.55	22	76.81
21	1400	80	7.1	22	74.18
22	1400	80	3.55	11	75.92
23	1400	160	3.55	22	74.84
24	2800	0	3.55	11	77.58
25	1400	0	3.55	22	71.23
26	0	80	0	11	81.56
27	1400	0	7.1	11	78.62
28	1400	160	7.1	11	76.61
29	0	160	3.55	11	79.51

Table S2. ANOVA analysis of the quadratic polynomial model.

Source	Sum of squares	Mean Square	F-Value	p-value
Model	554.21209	39.586578	21.860661	< 0.0001
A-Cl ⁻	115.44403	115.44403	63.750973	< 0.0001
B-SO ₄ ²⁻	32.901408	32.901408	18.168949	0.0008
C-NO ₃ ⁻	0.3852083	0.3852083	0.2127213	0.6517
D-HCO ₃ ⁻	315.8028	315.8028	174.3939	< 0.0001
AB	1.9321	1.9321	1.0669521	0.3191
AC	0.09	0.09	0.0497002	0.8268
AD	38.0689	38.0689	21.022562	0.0004
BC	2.7889	2.7889	1.5400977	0.2350
BD	22.420225	22.420225	12.380988	0.0034
CD	1.729225	1.729225	0.9549196	0.3451
A ²	13.131598	13.131598	7.2515844	0.0175
B ²	1.5043622	1.5043622	0.830745	0.3775
C ²	0.0126055	0.0126055	0.006961	0.9347
D ²	12.403641	12.403641	6.8495891	0.0203
Residual	25.352028	1.8108592	/	/
Lack of Fit	23.061908	2.3061908	4.0280699	0.0958
Pure Error	2.29012	0.57253	/	/
Cor Total	579.56412	/	/	/

Table S3. The Fukui Index of each atom for TC molecules.

Atom	f^-	f^0	f^+
1C	0.0236	0.0333	0.0431
2C	0.0237	0.0213	0.0190
3C	0.0284	0.0416	0.0549
4C	0.0883	0.0555	0.0227
5C	0.0136	0.0132	0.0127
6C	0.0440	0.0312	0.0184
7C	0.0344	0.0403	0.0461
8C	0.0369	0.0245	0.0121
9C	0.0418	0.0380	0.0341
10C	0.0158	0.0141	0.0125
11C	0.0303	0.0269	0.0235
12C	0.0064	0.0072	0.0079

13H	0.0251	0.0191	0.0131
14H	0.0179	0.0151	0.0123
15H	0.0100	0.0090	0.0079
16H	0.0133	0.0123	0.0114
17C	0.0387	0.0311	0.0235
18C	0.0213	0.0303	0.0393
19C	0.0055	0.0125	0.0195
20C	0.0169	0.0329	0.0488
21C	0.0678	0.0513	0.0347
22C	0.0242	0.0408	0.0575
23O	0.0345	0.0299	0.0253
24H	0.0132	0.0115	0.0098
25O	0.0226	0.0225	0.0224
26O	0.0286	0.0330	0.0374
27H	0.0095	0.0117	0.0139
28O	0.0323	0.0386	0.0448
29O	0.0126	0.0258	0.0389
30H	0.0089	0.0141	0.0194
31C	0.0127	0.0120	0.0113
32N	0.0111	0.0101	0.0092
33H	0.0058	0.0061	0.0065
34H	0.0070	0.0068	0.0066
35O	0.0205	0.0187	0.0168
36O	0.0255	0.0371	0.0488
37H	0.0088	0.0111	0.0134
38N	0.0073	0.0061	0.0048
39C	0.0078	0.0067	0.0056
40H	0.0080	0.0068	0.0056
41H	0.0067	0.0059	0.0050
42H	0.0064	0.0056	0.0048
43C	0.0087	0.0072	0.0057
44H	0.0074	0.0063	0.0053
45H	0.0076	0.0065	0.0055
46H	0.0064	0.0057	0.0049
47C	0.0090	0.0091	0.0093
48H	0.0071	0.0069	0.0066

49H	0.0080	0.0082	0.0083
50H	0.0058	0.0058	0.0058
51O	0.0107	0.0109	0.0112
52H	0.0065	0.0068	0.0070

Table S4. The charge distribution and Fukui Index of TC molecules.

Atom	$q(N)$	$q(N+1)$	$q(N-1)$	f^0	f^-	f^+	CDD
1C	0.1310	0.0879	0.1547	0.0333	0.0236	0.0431	0.0195
2C	-0.0583	-0.0773	-0.0345	0.0213	0.0237	0.0190	-0.0048
3C	0.0184	-0.0366	0.0469	0.0416	0.0284	0.0549	0.0264
4C	-0.0659	-0.0887	0.0225	0.0555	0.0883	0.0227	-0.0656
5C	0.1142	0.1013	0.1279	0.0132	0.0136	0.0127	-0.0009
6C	-0.0548	-0.0733	-0.0108	0.0312	0.0440	0.0184	-0.0256
7C	0.0211	-0.0250	0.0557	0.0403	0.0344	0.0461	0.0117
8C	-0.0499	-0.0621	-0.0129	0.0245	0.0369	0.0121	-0.0248
9C	0.1270	0.0928	0.1689	0.0380	0.0418	0.0341	-0.0077
10C	-0.0375	-0.0501	-0.0216	0.0141	0.0158	0.0125	-0.0033
11C	0.0041	-0.0195	0.0345	0.0269	0.0303	0.0235	-0.0068
12C	0.0916	0.0836	0.0981	0.0072	0.0064	0.0079	0.0015
13H	0.0512	0.0380	0.0763	0.0191	0.0251	0.0131	-0.0120
14H	0.0453	0.0329	0.0633	0.0151	0.0179	0.0123	-0.0056
15H	0.0732	0.0651	0.0833	0.0090	0.0100	0.0079	-0.0021
16H	0.0708	0.0594	0.0842	0.0123	0.0133	0.0114	-0.0019
17C	-0.0802	-0.1038	-0.0414	0.0311	0.0387	0.0235	-0.0152
18C	0.1290	0.0896	0.1504	0.0303	0.0213	0.0393	0.0180
19C	0.0832	0.0637	0.0889	0.0125	0.0055	0.0195	0.0139
20C	0.0096	-0.0393	0.0266	0.0329	0.0169	0.0488	0.0319
21C	0.0128	-0.0220	0.0807	0.0513	0.0678	0.0347	-0.0331
22C	0.1197	0.0622	0.1440	0.0408	0.0242	0.0575	0.0333
23O	-0.1535	-0.1788	-0.1188	0.0299	0.0345	0.0253	-0.0093
24H	0.2148	0.2049	0.2281	0.0115	0.0132	0.0098	-0.0034
25O	-0.3757	-0.3982	-0.3530	0.0225	0.0226	0.0224	-0.0002
26O	-0.1764	-0.2139	-0.1477	0.0330	0.0286	0.0374	0.0087
27H	0.1166	0.1027	0.1262	0.0117	0.0095	0.0139	0.0044

28O	-0.2227	-0.2676	-0.1903	0.0386	0.0323	0.0448	0.0126
29O	-0.2255	-0.2646	-0.2128	0.0258	0.0126	0.0389	0.0263
30H	0.1786	0.1591	0.1876	0.0141	0.0089	0.0194	0.0105
31C	0.1372	0.1258	0.1500	0.0120	0.0127	0.0113	-0.0014
32N	-0.1435	-0.1528	-0.1324	0.0101	0.0111	0.0092	-0.0018
33H	0.0987	0.0922	0.1046	0.0061	0.0058	0.0065	0.0006
34H	0.1383	0.1316	0.1454	0.0068	0.0070	0.0066	-0.0004
35O	-0.4331	-0.4500	-0.4124	0.0187	0.0205	0.0168	-0.0037
36O	-0.1793	-0.2282	-0.1537	0.0371	0.0255	0.0488	0.0233
37H	0.1379	0.1244	0.1467	0.0111	0.0088	0.0134	0.0046
38N	-0.0469	-0.0518	-0.0395	0.0061	0.0073	0.0048	-0.0024
39C	-0.0315	0.0372	-0.0235	0.0067	0.0078	0.0056	-0.0022
40H	0.0447	0.0390	0.0528	0.0068	0.0080	0.0056	-0.0024
41H	0.0341	0.0290	0.0409	0.0059	0.0067	0.0050	-0.0017
42H	0.0444	0.0395	0.0509	0.0056	0.0064	0.0048	-0.0016
43C	-0.0308	-0.0366	-0.0220	0.0072	0.0087	0.0057	-0.0029
44H	0.0343	0.0289	0.0418	0.0063	0.0074	0.0053	-0.0021
45H	0.0452	0.0395	0.0528	0.0065	0.0076	0.0055	-0.0021
46H	0.0439	0.0389	0.0505	0.0057	0.0064	0.0049	-0.0015
47C	-0.0788	-0.0882	-0.0697	0.0091	0.0090	0.0093	0.0003
48H	0.0420	0.0353	0.0492	0.0069	0.0071	0.0066	-0.0005
49H	0.0476	0.0392	0.0557	0.0082	0.0080	0.0083	0.0004
50H	0.0444	0.0385	0.0503	0.0058	0.0058	0.0058	0.0000
51O	-0.2404	-0.2517	-0.2296	0.0109	0.0107	0.0112	0.0006
52H	0.1796	0.1725	0.1862	0.0068	0.0065	0.0070	0.0004
